

Room-Temperature Ferromagnetism of Cu-Doped ZnO Films Probed by Soft X-Ray Magnetic Circular Dichroism

T. S. Heng,¹ D.-C. Qi,^{2,3} T. Berlijn,^{4,5} J. B. Yi,¹ K. S. Yang,^{3,6} Y. Dai,⁶ Y. P. Feng,³ I. Santos,^{2,7} C. Sánchez-Hanke,⁸ X. Y. Gao,³ Andrew T. S. Wee,³ W. Ku,^{4,5} J. Ding,^{2,1,*} and A. Rusydi^{2,3,9,†}

¹*Department of Materials Science and Engineering, National University of Singapore, 7 Engineering Drive 1, Singapore 117574, Singapore*

²*NanoCore, National University of Singapore, Singapore 117576, Singapore*

³*Department of Physics, National University of Singapore, 2 Science Drive 3, Singapore 117542, Singapore*

⁴*CMPMSD, Brookhaven National Laboratory, Upton, New York 11973, USA*

⁵*Department of Physics and Astronomy, SUNY Stony Brook, Stony Brook, New York 11794, USA*

⁶*School of Physics, Shandong University, Jinan 250100, People's Republic of China*

⁷*Department of Chemistry, National University of Singapore, 3 Science Drive 3, Singapore 117543, Singapore*

⁸*National Synchrotron Light Source, Brookhaven National Laboratory, Upton, New York 11973, USA*

⁹*Singapore Synchrotron Light Source, National University of Singapore, 5 Research Link, Singapore 117603, Singapore*
(Received 24 November 2009; published 8 November 2010)

We report direct evidence of room-temperature ferromagnetic ordering in O-deficient ZnO:Cu films by using soft x-ray magnetic circular dichroism and x-ray absorption. Our measurements have revealed unambiguously two distinct features of Cu atoms associated with (i) magnetically ordered Cu ions present only in the oxygen-deficient samples and (ii) magnetically disordered *regular* Cu²⁺ ions present in all the samples. We find that a sufficient amount of both oxygen vacancies (V_O) and Cu impurities is essential to the observed ferromagnetism, and a non-negligible portion of Cu impurities is uninvolved in the magnetic order. Based on first-principles calculations, we propose a microscopic “indirect double-exchange” model, in which alignments of localized large moments of Cu in the vicinity of the V_O are mediated by the large-sized vacancy orbitals.

DOI: 10.1103/PhysRevLett.105.207201

PACS numbers: 75.70.-i, 75.30.-m, 75.50.Pp, 78.20.Ls

In recent years, there have been more startling discoveries in diluted magnetic semiconductors (DMSs) [1]—achieving possible room-temperature ferromagnetism in undoped (i.e., HfO₂ [2], ZnO [3], and TiO₂ [4]) and nontransition-metal-doped (i.e., ZnO:C [5], ZnO:Ga [6], and SrO:N [7]) systems. In light of these discoveries, there has been an emerging consensus that defects in DMS systems play critical roles in inducing or mediating ferromagnetism (FM) [8] despite the lack of direct experimental accesses on the nature and positions of these defects. ZnO-based material serves as a model for the oxide DMS system and is one of the most intensely studied system so far [9,10]. Copper-doped ZnO (ZnO:Cu) is particularly interesting [11–15]. While neither metallic Cu nor its oxides (CuO and Cu₂O) are ferromagnetic at 300 K, recent superconducting quantum interference device (SQUIDs) and vibrating sample magnetometer measurements [11,12] have suggested the existence of FM in ZnO:Cu. However, as pointed out by Ando [16], a SQUID is necessary but not sufficient to reveal intrinsic FM. Thus, a more detailed study with an element-specific, magnetism-sensitive spectroscopic probe such as a soft x-ray magnetic circular dichroism (SXMCD) measurement is urgently needed [17].

In this Letter, we present the first direct evidence of room-temperature ferromagnetism in O-deficient ZnO:Cu film by using SXMCD and x-ray absorption (XAS). We

have revealed unambiguously two distinct sites of Cu associated with magnetically ordered Cu ions present in the vicinity of oxygen vacancies (V_O) and magnetically disordered regular Cu²⁺ ions. Furthermore, the magnetic polarization of O ions is found due to the presence of V_O , and their magnetic moments are strikingly opposed to those of the Cu ions. First-principles calculations were performed for the disordered system, and a microscopic “indirect double-exchange” model was proposed to explain all these key observations. Our results directly suggest the importance of Cu and V_O for inducing FM in the ZnO:Cu system.

ZnO:Cu thin films (doped with 2% of Cu and nominal thickness ~ 50 nm) with a prominent *c*-axis (002) texture were grown on an *X*-cut quartz substrate by the pulsed laser deposition technique at 350 °C. For detailed studies here, we chose three representing samples: (a) sample 1: an undoped ZnO film—which is used as a reference sample; (b) sample 2: 2% ZnO:Cu under an oxygen partial pressure (P_O) of 1×10^{-3} torr for O-rich conditions; and (c) sample 3: with P_O of 5×10^{-6} torr for O-deficient conditions. To study the Zn, O, and Cu distribution in ZnO:Cu films, we have performed secondary ion mass spectroscopy, energy dispersive spectroscopy, and cross-sectional transmission electron microscopy-energy dispersive spectroscopy analysis at various locations of our films. The results elucidate that Zn, O, and Cu are homogeneously distrib-

uted across our ZnO:Cu films, and no phase segregation or/and clustering were detected (cf. Figs. S1–S3 in Ref. [18]).

Figure 1 shows magnetic hysteresis loops taken at various temperatures for all three samples from the SQUID measurements. Sample 3 exhibits FM with a coercivity of 260 Oe and a saturated magnetic moment (M_s) of $0.5\mu_B/\text{Cu}$ (measured at 300 K) which keeps almost constant across its thickness from 40 to 200 nm. (cf. Fig. S4 in [18]). However, the M_s is dampened by $\sim 94\%$ to $0.03\mu_B/\text{Cu}$ for sample 2 (practically nonmagnetic). Note that no FM was observed in the undoped ZnO (sample 1). These SQUID results have shown that Cu doping and O-deficient conditions are two indispensable ingredients for observing FM in ZnO:Cu. As seen from the inset in Fig. 1, the M_s of sample 3 persists at $\sim 0.5\mu_B/\text{Cu}$ for the whole temperature range, showing the FM with a Curie temperature of 750 K, which is also reconfirmed by the Arrott plot and temperature-dependent inverse magnetic susceptibility curve (cf. Fig. S5 in [18]).

To correlate the observed magnetic properties with the local chemical and electronic state, x-ray photoemission spectroscopy, Raman, photoluminescence, and secondary ion mass spectroscopy analysis were carried out at various locations on the ZnO films (cf. Figs. S6–S8 in [18]). From a close inspection of the x-ray photoemission spectroscopy peak for Cu, d^{10} (Cu^{1+} -like) is dominant in sample 3 ($d^9 : d^{10} \approx 5:1$), whereas most Cu ions are in the d^9 (Cu^{2+} -like) state in sample 2 ($d^9 : d^{10} \approx 1:4$). Additionally, Raman spectra indicated the possible presence of defects in sample 3, e.g., Zn interstitial or/and V_O , whose intensity decreases with increasing O-partial pressure and vanishes after annealing in air. This phenomenon has been reconfirmed by photoluminescence analysis (not shown

here), showing the appearance of green emission centered at around 520 nm in sample 3. The above study has shown that the FM in sample 3 is associated with the large amount of Cu^{1+} -like ions and the possible presence of defects. The secondary ion mass spectroscopy study estimated the V_O concentration of sample 3 is about $0.9 \pm 0.1\%$ [18].

Figures 2(a) and 2(b) show the XAS spectra at O K ($\text{O } 1s \rightarrow 2p$) and Cu $L_{3,2}$ ($\text{Cu } 2p \rightarrow 3d$) edges for different ZnO samples, respectively. Because of hybridizations with other states, the spectra of the O K edge displays broad features above the absorption edge [Fig. 2(a)]. By properly normalizing the absorption spectra, we have found that the spectral weight decreases for both sample 2 and sample 3 as compared to the reference sample 1, where sample 3 exhibits a larger decrease in intensity than sample 2. Since the intensity of XAS spectra is proportional to the density of unoccupied states and the oxygen concentration, the spectral weight decrease upon doping is a direct reflection of a decrease in the number of O $2p$ holes and an increased number of electrons, both linked to the occurrence of V_O . For a rough estimate using the spectral weight variation of the O K edge, the V_O in sample 2 is at a lower level, while V_O in sample 3 is about 1%. In contrast, the Zn L edges of all samples (cf. Fig. S10 in [18]) closely resemble each other, indicating that the doping of Cu and V_O barely influences the electronic states of Zn and thereby ruling out the existence of Zn interstitials.

The Cu $L_{3,2}$ edges provide important information about the electronic structures of Cu impurities as shown in Fig. 2(b). In comparison with the standard XAS spectra of the Cu L_3 edge in CuO and Cu_2O [19], we attribute the excitation at 931.6 eV to regular Cu^{2+} ions in d^9 configuration that dominate sample 2. By contrast, in sample 3 with more V_O , the spectral weight of the 931.6 eV peak decreases significantly, while a new peak appears at 935 eV with approximately 4 times higher intensity. Apparently, this new feature in sample 3 is directly related to the introduction of the V_O or, more precisely, strong influence of V_O on the majority of Cu impurities in the sample, making them carry a mixed d^9 and d^{10} character. Nonetheless, the remaining structure at 931.6 eV indicates that some portion of the Cu impurities remain unaffected by V_O .

The center of the study is the SXMCD results as shown in Figs. 2(c) and 2(d). SXMCD is a direct and powerful tool that can explicitly probe the element-specific local magnetism, providing direct and strong proof whether a material is a genuinely DMS [17]. Strong SXMCD signals of the Cu $L_{3,2}$ edges and O K edge are obtained for sample 3, whereas virtually no SXMCD signals are observed in sample 2 (not shown here), in good agreement with the SQUID results. Important to note here is that the SXMCD signals observed here essentially correspond to the remnant (zero-field) magnetization inherent to the samples, thus eliminating possible paramagnetic contribu-

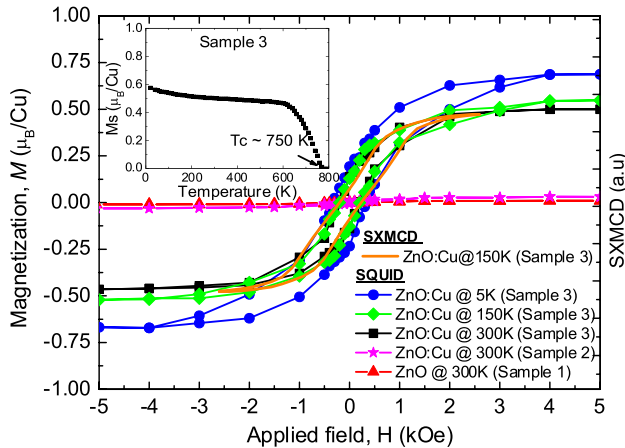


FIG. 1 (color online). Magnetic hysteresis loops for ZnO (controlled sample) and ZnO:Cu films at varying processing conditions and measurement temperatures. Inset: Temperature dependence of saturated magnetization (M_s - T) of the oxygen-deficient ZnO:Cu film (sample 3), showing the Curie temperature of 750 K. The magnetic hysteresis loop obtained from the SXMCD signal is shown as a dark brown line.

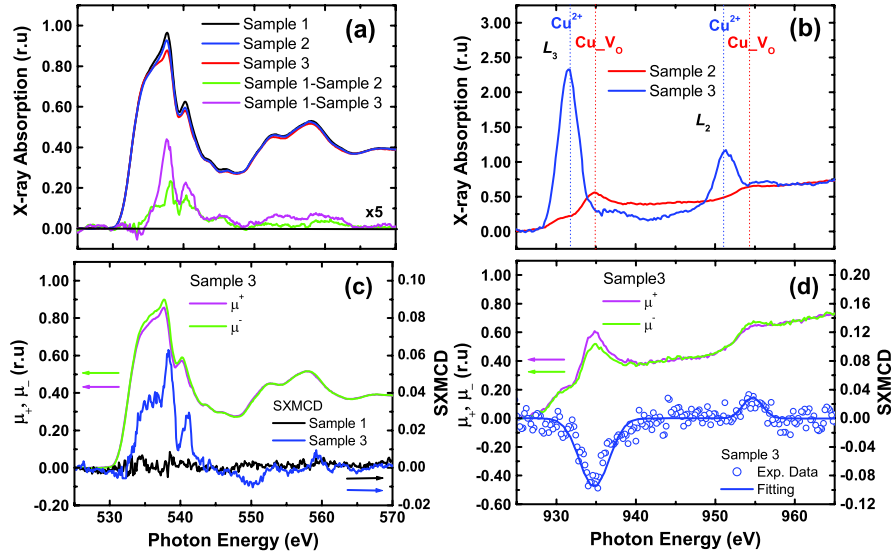


FIG. 2 (color online). XAS of the ZnO samples at (a) the O K edge with the difference spectra and (b) Cu $L_{3,2}$ edges. The O K edge and Cu $L_{3,2}$ edges XAS of sample 3 for two opposite magnetization directions relative to the fixed photon helicity (μ^+ and μ^-) are shown in (c) and (d), respectively, with their corresponding SXMCD signal ($\mu^- - \mu^+$) at the bottom (right scale). All XAS spectra are normalized below and above the absorption edge.

tions [20]. Consequently, the observed ferromagnetic ordering at room temperature can be explicitly associated with the magnetic polarization on both the O $2p$ and Cu $3d$ states.

Most strikingly, SXMCD measurement at Cu $L_{3,2}$ edges [Fig. 2(d)] reveals that these two types of Cu impurities play entirely different roles in the magnetism. The regular Cu^{2+} impurities show surprisingly no observable SXMCD signals at 931.6 eV in both sample 2 and sample 3. That is, the well-defined large local moments of isolated Cu^{2+} impurities are essentially magnetically disordered even in the magnetic sample 3 and thus are not responsible for the zero-field FM. Note that the contribution of paramagnetic isolated Cu^{2+} to the hysteresis loop in Fig. 1 is negligibly small as compared to the ferromagnetic substance due to extremely small magnetic permeability in the paramagnetic substance ($\ll 1$). By sharp contrast, the V_{O} -coupled Cu impurities show a strong SXMCD signal at 935 eV. Furthermore, the magnetic hysteresis loop obtained by using the 935 eV SXMCD signal closely resembles the SQUID hysteresis loop (Fig. 1), indicating that the FM originates from those V_{O} -coupled Cu impurities (Cu_-V_{O}).

Further insights into the microscopic mechanism of FM are obtained via the O K edge SXMCD. As shown in Fig. 2(c), the predominant SXMCD signal resides in the region between 532 and 545 eV which is mainly associated with the O $2p$ hybridization with dispersive Zn $4s$ /Cu $3d4sp$ states [21,22]. To have a direct representation of the unoccupied O $2p$ states related to V_{O} , we compute the O K edge difference spectra between doped and undoped samples in Fig. 2(a). By comparison, one immediately observes the similar structures of SXMCD and the XAS difference spectrum for sample 3, manifesting the close

relation between the magnetic polarization in O and the V_{O} orbitals. Moreover, the SXMCD spectrum exhibits additional structures at low photon energy around 535 eV which is believed to originate from hybridization with Cu $3d$ states [e.g., the peak at 935 eV in Fig. 2(b)]. Hence, there is intimate interplay between V_{O} and surrounding V_{O} -coupled Cu ions, which plays a decisive role in inducing the magnetic ordering in ZnO:Cu. It is important to note the fact that we have seen the SXMCD signals at both the Cu L edge and the O K edge is strong evidence of the $s - pd$ interactions in this system.

Interestingly, the SXMCD signals show opposite signs in the O K edge and Cu L_3 edge. By applying the

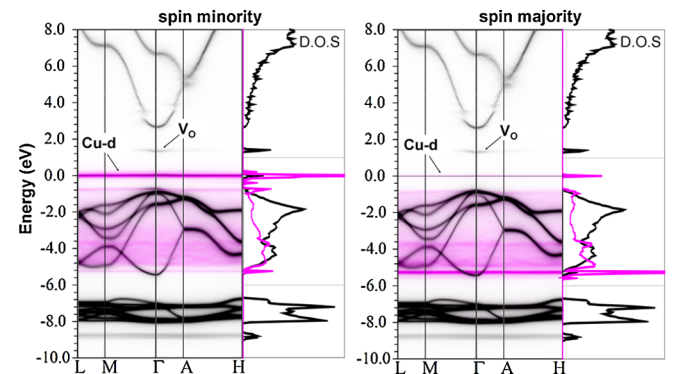


FIG. 3 (color online). First-principles calculations of disordered ZnO with 2% Cu impurities and $\sim 1\%$ of V_{O} within the “LDA + U ” approximation. The intensity of the Cu- $3d$ band (pink) has been multiplied by a factor of 40 to make the impurity states more visible. For the same reason, the intensity of the density of states panels $[-10, -6 \text{ eV}]$ and $[1, 8 \text{ eV}]$ have been rescaled by a factor of 1/3 and 5, respectively.

SXMCD sum rules, the opposite polarity of the Cu L_3 and the O K edge SXMCD suggests an antiparallel alignment of the magnetic moments between Cu and O ions (ferrimagnetism-type exchange coupling), while the material displays a macroscopic FM due to the alignment of Cu magnetic moments. This nontrivial observation introduces a stringent constraint to any potential microscopic explanation of the magnetism in this material.

To understand better these clear experimental observations, we performed first-principles calculations of quasi-particle dispersion of disordered ZnO with 2% Cu impurities and $\sim 1\%$ of V_O within the ‘‘LDA + U ’’ approximation [23] ($U = 8$ eV, $J = 0.9$ eV for both Zn and Cu atoms), solving the Hamiltonian only within the low-energy Hilbert space, defined via the first-principles Wannier functions [18]. The result of the calculation is shown in Fig. 3. The spectral functions are averaged over a number of configurations of various sizes and shapes (containing 94.8 Zn atoms on average), in which the Cu atoms have random positions and the Cu electrons have random spin orientations, such that their average moment matches the experimentally observed value. In great contrast to the standard small-cell calculations without disorder, our results demonstrate several important and novel features relevant to the physics of interest here. First, Cu-3d levels are found to be flat with a spectral weight that is constant in k space, indicating that the Cu impurity orbitals are extremely localized. Second, a nondegenerate V_O orbital is found inside the band gap about 1.5 eV below the conduction band. The intensity of V_O centers near the Γ point and spreads in k space with a FWHM of $\sim \frac{1}{5}\Gamma M$, indicating a large orbital size with a radius of about 2.25 times the lattice constant [18]. Obviously, the V_O orbital is much less localized than the Cu ones and is thus more efficient in communicating with each other. Interestingly, this size

agrees very well with the one estimated from a simple model with input from our experimental data [18]. Third, the upper Hubbard level of Cu (at the chemical potential) and the lower Hubbard level (at -5 eV) show incomplete spin polarization, reflecting the existence of both isolated Cu with disordered moment and Cu in the vicinity of V_O with ordered moments. One key message from our calculations is that the V_O level lies ~ 1.8 eV above the upper Hubbard level of Cu. This leads to a definite conclusion that, rather than staying in the V_O orbitals, the doped electrons associated with the V_O would fill the 3d orbitals of the surrounding Cu impurities, making them closer to d^{10} configuration.

Therefore, we propose an indirect double-exchange model to explain the FM in ZnO:Cu (Fig. 4). Consistent with previous studies [24], our first-principles calculation shows that each V_O introduces one localized orbital with a large size and two doped electrons. As illustrated in Fig. 4(b), to benefit from the kinetic energy, the doped electrons would hop between different Cu impurities via the V_O orbitals, causing the Cu impurities connected via the V_O orbitals to align ferromagnetically. This is a natural extension of the well known ‘‘double-exchange effect’’ but now mediated by the large V_O orbitals. Therefore, a long-range ferromagnetic order would develop provided that there is a sufficient amount of V_O larger than the percolation threshold, as is exactly the case in our O-deficient sample 3. That is, in this model Cu moments in the proximity of the V_O align parallel to each other, mediated via the V_O orbitals.

This simple model also explains very naturally the two key observations of our SXMCD measurement. First, note that Cu impurities residing outside the range of V_O will remain magnetically disordered in purely d^9 configuration due to the lack of the indirect double-exchange coupling channel. On the other hand, most of the Cu impurities in the proximity of V_O ($Cu_{-}V_O$) receive the doped electrons and behave more like d^{10} (Cu^{1+} -like), however, with a mixture of d^9 . This explains why the new V_O -coupled Cu structure at ~ 935 eV shows dichroism, while the isolated Cu structure at ~ 931.4 eV does not. Second, from Fig. 4(b) it is obvious that the V_O orbitals will pick up a magnetic moment opposite to that of the Cu impurities. Since the V_O orbital consists of superposition of primarily Zn- s and O- p orbitals, the SXMCD with the O- K edge measuring the V_O orbitals would show opposite dichroism to the Cu L -edge measurement, exactly as reported above. In essence, V_O mediates the alignment of local moments of Cu impurities and in turn picks up an antiparallel moment in the process. Meanwhile, the relatively wide energy distribution of the O K edge SXMCD spectra is directly connected to the itinerant nature of the hopping electrons participating in the ferromagnetic exchange interaction as depicted in our model. Because of the large size of the V_O orbital, the oxygen atoms within the

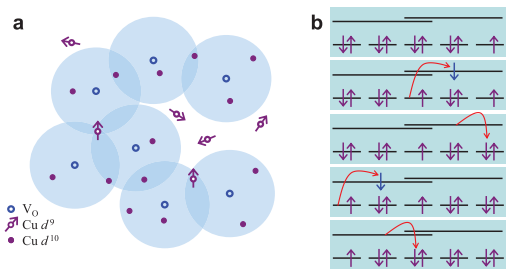


FIG. 4 (color online). Schematic illustration of the indirect double-exchange model mediated by V_O . In (a), the light blue circles represent the size of the vacancy orbitals within which Cu atoms receive two doped electrons per V_O and their moments are aligned ferromagnetically. In (b), microscopic picture of one example of the indirect double-exchange process with snapshots in (i)–(v). The long lines represent two overlapped V_O orbitals. The short lines below represent individual Cu ions inside the blue circles (V_O orbitals) with their upper Hubbard band fully filled (d^{10}) or partially filled (d^9). The red arrows illustrate the spin-polarized electron hopping process.

range of V_O are expected to be magnetically polarized. This may lead to a SXMCD signal for a large energy range within which the oxygen orbitals exist, in contrast to the much narrower energy range in the Cu L edge SXMCD simply because of the much more localized Cu $3d$ orbitals.

In conclusion, we have observed room-temperature ferromagnetism in ZnO:Cu film with the coexistence of Cu 2 at. % doping and about 1% (or less) of V_O under optimal conditions. Using SXMCD and XAS, we have found two distinct Cu impurities in the magnetic ZnO:Cu, isolated unordered Cu^{2+} ions, and Cu impurities coupled to V_O that order ferromagnetically. In addition, the magnetic moments of O are found opposite to Cu. Based on first-principles calculations, we propose an indirect double-exchange model for the FM in ZnO:Cu that explains our main experimental findings.

This work was supported by NRF-CRP Grants No. NRF-G-CRP 2007-05 and No. NRF2008NRF-CRP002-024, NUS YIA, NUS Cross Faculty, FRC, DOE Grant No. DE-AC02-98CH10886, and CMSN and NNSFC Grant No. 10774091. This work was partly performed at SSLS under NUS Core Support Grants No. C-380-003-003-001, No. A*STAR/MOE RP 3979908M, and No. A*STAR 12 105 0038.

*msedingj@nus.edu.sg

†phyandri@nus.edu.sg

[1] T. Dietl *et al.*, *Science* **287**, 1019 (2000).

[2] M. Venkatesan *et al.*, *Nature (London)* **430**, 630 (2004).

- [3] Q. Xu *et al.*, *Appl. Phys. Lett.* **92**, 082508 (2008).
 [4] N.H. Hong *et al.*, *Phys. Rev. B* **73**, 132404 (2006).
 [5] H. Pan *et al.*, *Phys. Rev. Lett.* **99**, 127201 (2007).
 [6] V. Bhosle *et al.*, *Appl. Phys. Lett.* **93**, 021912 (2008).
 [7] I. S. Elfimov *et al.*, *Phys. Rev. Lett.* **98**, 137202 (2007).
 [8] J. M. D. Coey *et al.*, *Nature Mater.* **4**, 173 (2005).
 [9] C. Liu *et al.*, *J. Mater. Sci.* **16**, 555 (2005).
 [10] J. M. D. Coey, *Curr. Opin. Solid State Mater. Sci.* **10**, 83 (2006).
 [11] D. B. Buchholz *et al.*, *Appl. Phys. Lett.* **87**, 082504 (2005).
 [12] T. S. Heng *et al.*, *J. Appl. Phys.* **99**, 086101 (2006).
 [13] L.-H. Ye, A. J. Freeman, and B. Delley, *Phys. Rev. B* **73**, 033203 (2006).
 [14] Q. Ma, D. B. Buchholz, and R. P. H. Chang, *Phys. Rev. B* **78**, 214429 (2008).
 [15] L. M. Huang, A. L. Rosa, and R. Ahuja, *Phys. Rev. B* **74**, 075206 (2006).
 [16] K. Ando, *Science* **312**, 1883 (2006).
 [17] P. Carra *et al.*, *Phys. Rev. Lett.* **70**, 694 (1993); B. T. Thole *et al.*, *Phys. Rev. Lett.* **68**, 1943 (1992); J. Stöhr, *J. Magn. Magn. Mater.* **200**, 470 (1999).
 [18] See supplementary material at <http://link.aps.org/supplemental/10.1103/PhysRevLett.105.207201> for details of sample preparation, material characterizations, and theoretical calculations.
 [19] M. Grioni *et al.*, *Phys. Rev. B* **45**, 3309 (1992).
 [20] D. J. Keavney *et al.*, *Appl. Phys. Lett.* **91**, 012501 (2007).
 [21] P. Thakur *et al.*, *Appl. Phys. Lett.* **91**, 162503 (2007).
 [22] S. Krishnamurthy *et al.*, *J. Appl. Phys.* **99**, 08M111 (2006).
 [23] V. I. Anisimov *et al.*, *Phys. Rev. B* **48**, 16929 (1993).
 [24] I. S. Elfimov, S. Yunoki, and G. A. Sawatzky, *Phys. Rev. Lett.* **89**, 216403 (2002).